

Approximate analysis of hydrofoil material impact on cavitation inception

E. L. Amromin

Mechmath LLC, Federal Way, WA 98003, USA; E-mail: amromin@aol.com

ABSTRACT

This study was motivated by results of the experiments [1] with hydrofoils Cav2003 fabricated from diverse metals and tested in the same water tunnel. A substantial difference (shown in Fig.1) in their cavitation inception and desinence numbers was observed.

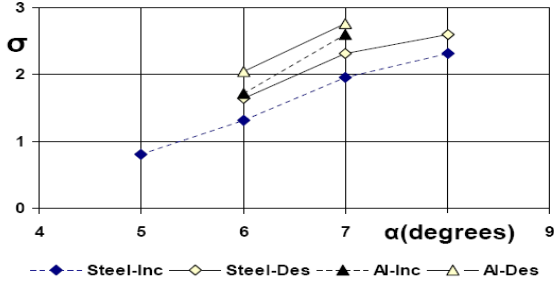


Fig 1 Observed cavitation inception (Inc) and desinence (Des) numbers for Aluminum (Al) and Steel hydrofoils

It was already noted [2] that blade cavitation inception may be influenced by vibration. This study provides a multi-step analysis of the hypothesis of vibration impact on cavitation inception in experiments [1] and gives some estimations of the effect level. First, the hydrofoil spanwise deformations in water tunnel turbulent incoming flow are found. Second, its chordwise deformations in this flow are found. Third, the pressure around hydrofoils vibrating at resonance frequencies is computed. Finally, cavitation inception and desinence numbers are computed for the actual values of the hydrofoil chord C and the incoming flow speed U_0 .

The spanwise vibration can be found using strong coupling of the equations for beam deformations $\{V, \theta\}$

$$\frac{E^* I}{U^2} \frac{\partial^4 V}{\partial z^4} - (\rho S + m_1)(V + X\theta)St^2 - \hat{\rho} \int_0^C F dx = 0,$$

$$\frac{G^*}{U^2} \frac{\partial}{\partial z} \left(J \frac{\partial \theta}{\partial z} \right) + St^2 [\rho SXV + (I_\theta + m_2)\theta] - \hat{\rho} \int_0^C \left(x - \frac{C}{2} \right) F dx = 0$$

similar to employed in [3] and Birnbaum equation for load pulsation γ regularized (as in [4]) to the form

$$\gamma + \frac{i\omega\Psi(x)}{\pi} \int_0^C \int_0^{\frac{C}{\pi}} \frac{e^{i\omega(\xi - \tau)}}{\omega(\tau - \xi)} \int_0^\infty \frac{e^{i\chi} d\chi}{\chi} d\tau \frac{d\xi}{\Psi(\xi)}$$

$$- \frac{i\omega\Psi(x)}{\pi} \int_0^C \left[\left(\xi - \frac{C}{2} \right) \theta + V \right] \frac{d\xi}{\Psi(\xi)} = - \frac{\Psi(x)}{\pi} \int_0^C \frac{\partial \Phi_1}{\partial y} \frac{d\xi}{\Psi(\xi)}$$

Here E^* and G^* are complex elasticity modules; ρ and $\hat{\rho}$ are densities of metal and water; I, J, I_θ are section

inertia moments, S is its area; m_1, m_2 are section added masses; V and θ are bending and torsion deformations;

$$F = \gamma U_0 - i\omega \int_0^x \gamma d\xi; U = \sqrt{1 - Cp}; \Psi(x) = \sqrt{C/x - 1};$$

$St = \omega C / U_0$; ω is perturbation frequency. The solutions of the above equations for a very soft ($\text{Real}\{E^*\} = 3\text{Mpa}$) hydrofoil of aspect ratio $\lambda = 1.27$ gave the first bending resonance at 60Hz, whereas loose coupling computations [3] gave it at 59Hz for this hydrofoil with a very small cavity (cavitation can reduce this resonance frequency). Some characteristics of spanwise bending vibration of hydrofoils Cav2003 of $C = 0.08\text{m}$, and the aspect ratio $\lambda = 2.35$ at $U_0 = 10\text{m/s}$ are shown in Fig.2; these results are normalized by $U_i = \chi U_0$, where χ is turbulence intensity. The inflow turbulence spectrum was selected with regards to usual data for water tunnels.

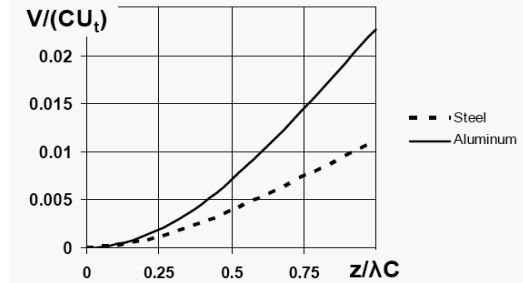


Fig 2 Hydrofoil spanwise deformations at resonances

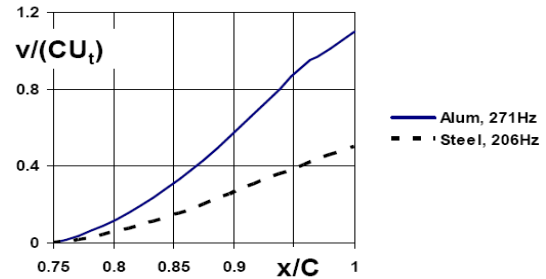


Fig 3 Hydrofoil chordwise deformations at resonances

Like in [3], torsion deformations in the considered frequency band ($f = \omega / 2\pi < 500\text{Hz}$) were negligible here. The chordwise deformation was computed using first and third of the above equations with $\theta = 0$ and the value of V at $x = C/2$ found during determination of spanwise deformations. As seen in Fig.3, only the trailing part of the hydrofoil undergoes substantial chordwise deformations, and these deformations depend on the hydrofoil material and real thickness of the trailing edge (it does not go to zero because it is not absolutely sharp).

Determination of σ_i and σ_d first requires computation of pressure over the hydrofoil vibrating in the unsteady flow. The issue for such computation is in the insufficient information on the real water tunnel incoming flow. Neither the turbulence magnitude spectrum, nor phases of its harmonic are usually known. So, only solutions for single-frequency inflows at the resonance frequencies would be free of arbitrary assumptions and usable for the further estimations. Data from such solutions for $\chi=0.01$ are presented in Fig.4.

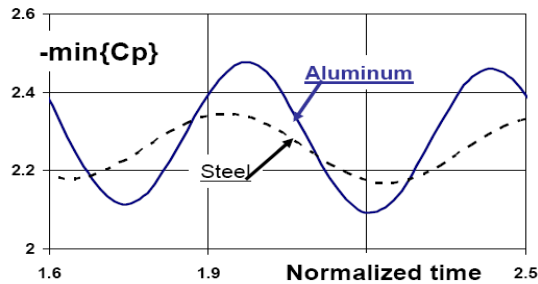


Fig 4 Histories of Cp minima at $\alpha=6^\circ$ (a) for hydrofoils made from different materials.

The following computations of σ_d are based on the earlier described model of sheet cavitation in viscous fluid [5] that also takes into account surface tension effect and considers the maximum of σ for a quasi-steady sheet cavity at given C and Re as σ_d . For hydrofoil cavitation inception, the computed σ_i corresponds to the pressure within a stable spherical bubble in the laminar separation zone at the hydrofoil leading edge (also as in [5]). Such quasi-steady approach is acceptable for the considered resonance frequencies because the corresponding periods are substantially greater than the time necessary for the cavity growth from a bubble.

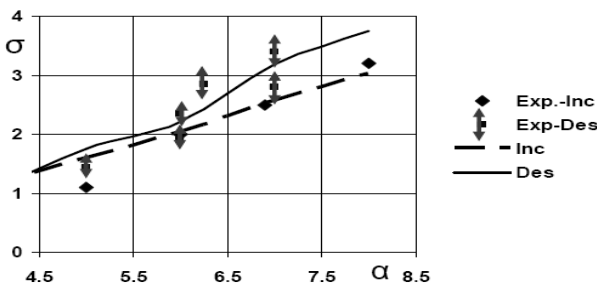


Fig 5 Computed [5] for rigid Cav2003 and measured [6] cavitation inception and desinence numbers

Computed σ_d for Cav2003 is presented in Fig.5 among with measurements [6] and in Fig.6 among with measurements [1]. There is no coincidence, but on the other hand, the data [1] are not very close to the data [6] for Cav2003 hydrofoil tested in another facility. The ability of computed results to follow the experimental trends is shown in general, but because of the mentioned insufficiency of information on the incoming flow, there

is no possibility to directly apply computations to prediction of the material effect on cavitation inception and desinence. Instead the material influence can be estimated by comparison of some ratios.

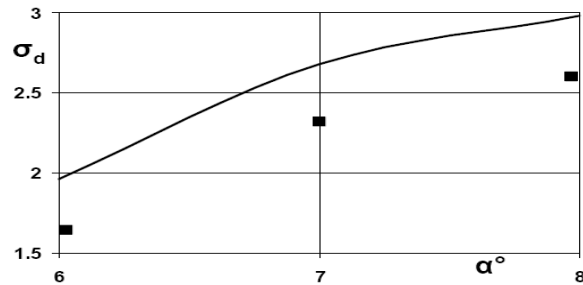


Fig 6 Comparison of computed (line) and measured (squares) σ_d [1].

Let us introduce $d\sigma$ as the difference between cavitation inception (or desinence) numbers for the aluminum hydrofoil and the steel hydrofoil. Then ratios from Fig.7 can be considered for a qualitative criterion for the comparison of the presented numerical analysis and experimental data.

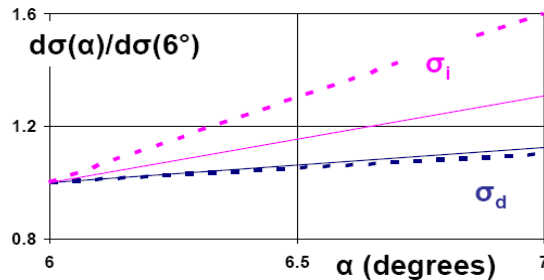


Fig 7 Hydrofoil material impact on σ_d and σ_i ; dashed lines show data [1], solid – numerical results

The provided numerical analysis manifests that the hydrofoil/blade material can substantially impact its cavitation and desinence just due to the hydroelastic effects. This impact should be considered among other factors listed (for example, in [7]) as influencing cavitation inception and the parameters predetermining the impact should be recorded.

REFERENCES

- [1] Williams M., Kawakami E, Amromin E, Arndt R 2009 7th Int. Symp. Cavitation, Ann Arbor
- [2] Ausoni P, Farhat M, Escaler X, Egusquiza E, Avellan F 2007 ASME J. Fluids Eng. **129** 966-973
- [3] Akcabay D T, Chae E J, Young Y L, Ducoin A, Astolfi JA 2014 J. Fl. Structures **49** 463-484
- [4] Amromin E L, Kovinskaya S I 2000 J. Fl. Structures **14** 735-747
- [5] Amromin E L 2014 ASME J. Fluids Eng. **136** 081303
- [6] Coutier-Delgosha O, Deniset F, Astolfi J A, Leroux J-B 2007 ASME J. Fluids Eng. **129** 279-292
- [7] Gindroz B, Billet M L 1998 ASME J. Fluids Eng. **120** 171-178